Proceedings of ISFOG 2025
5TH INTERNATIONAL SYMPOSIUM ON
FRONTIERS IN OFFSHORE GEOTECHNICS
Nantes, France | June 9-13 2025
© 2025 the Authors
ISBN 978-2-85782-758-0

Drainage Conditions Around Monopiles in Sand Under Cyclic Loading

K. Kaltekis*
Geowynd, London, UK

S. Whyte, C. Piatti
Geowynd, London, UK

E. Skoufaki, L.R. Christiansen
Vattenfall, London, UK

**kks@geowynd.com (corresponding author)*

ABSTRACT: Sand, and especially silty sand, is highly degradable under cycles of undrained loading, hence the degree of drainage in a storm fully controls the required pile penetration depth in sand dominated profiles. Undrained cyclic stress-strain curves, representing the equivalent accumulated strain for storm loading at different stress mobilizations, are typically employed for monopile design analysis in sand dominated units based on interpretation of cyclic contour diagrams using site-specific storm Markov matrix data. Such design approaches can also consider the effect of drainage occurring concurrently with the excess pore pressure (epp) generation during each load parcel. Conservative drainage assumptions are typically employed within simplified analytical or empirical models to estimate the degree of epp dissipation. This paper reviews the drainage characteristics (epp build-up and dissipation) around a laterally loaded monopile. In particular, a number of key factors influencing the epp dissipation (load utilisation, pile embedment ratio, sand permeability and presence of a shallow clay layer) were investigated. Fully coupled flow-deformation finite element analyses were performed using a soil constitutive model, calibrated against cyclic contour diagrams from a North Sea dense sand to generate a representative pore pressure field, for a given number of cycles, prior to running the dissipation stage to examine the storm drainage time.
The paper shows that the drainage characteristics of the system can have a substantial impact on the storm drainage time and hence the monopile response. The evolution of pore pressure ratio over time is presented which can be used to inform the degree of epp dissipation that can be considered during a storm for the various sensitivity cases. It is also shown how these results can be used to calibrate an analytical radial dissipation model within the design framework of cyclic envelope stress-strain curve development.

Keywords: FEA; cyclic loading; sand; monopile; drainage

1 INTRODUCTION

Soils that classify as “SAND” are typically treated as drained, though this assumption is unlikely to be valid for large diameter monopiles, particularly under cyclic loading. Sand, and even more so silty sand, is highly degradable under a few cycles of undrained loading. Therefore, the degree of drainage in a storm fully controls the pile penetration depth (PPD) in sand dominated soil profiles. Such equivalent undrained cyclic stress-strain curves are typically employed for monopile design analysis in sand dominated units, based on interpretation of cyclic contour diagrams, using the site-specific storm Markov matrix data.

A cyclic envelope stress-strain curve, also termed the N_{eq} stress-strain curve (Andersen, 2015), which represents the equivalent accumulated strain for storm loading at different stress mobilisations, is a typical input for monopile design analysis. This N_{eq} curve gives the accumulated shear strains at an envelope of cyclic stress ratios for a given number of cycles considering fully undrained conditions. It can also entail the consideration of the effect of drainage occurring simultaneously with the excess pore pressure generation during each load parcel for the sand units to define an N_{eq} which only considers equivalent fully undrained cycles.

This study adopted a methodology in accordance with Andersen (2015) which includes a consolidation component comprising a circular disk with radial pore pressure dissipation based on dissipation diagrams (Figure 1). The (equivalent) drainage length (i.e. distance between the monopile sleeve and the free drainage boundary) is a key parameter in this simplified analytical radial dissipation analysis. A parametric study

with the use of fully coupled flow-deformation finite element analyses (FEA) was performed to investigate the influence of a number of key factors (load utilisation, pile embedment ratio, sand permeability and presence of a shallow clay layer) in the derivation of the equivalent drainage length.

2 APPROACH

The adopted approach included the following steps:

- Select a suitable constitutive model and calibrate it based on typical North Sea cyclic contour diagrams to a specific N_{eq} for pore pressure and shear strain accumulation.
- Perform 3D FEA undrained loading stage in Plaxis (2021), considering the calibrated N_{eq} cyclic constitutive model for two mobilisation levels of the ultimate load to generate a representative excess pore pressure field.
- Review the excess pore pressure bulb lateral extent (from the pile sleeve to $PPR \approx 0$, where PPR is the normalised pore pressure defined as $PPR = u/u_0$, where u is the excess pore pressure at a specific time interval and u_0 is the excess pore pressure for undrained loading) along the pile length.
- Perform 3D FEA consolidation stage for dissipation of the generated excess pore pressure field.
- Determine drainage times (t) for various PPR.
- For each pair of $t - PPR$ calculate the drainage length (α) in accordance with the analytical radial dissipation method from Andersen (2015) (see Figure 1) and determine the drainage length at the time of nearly full drainage.

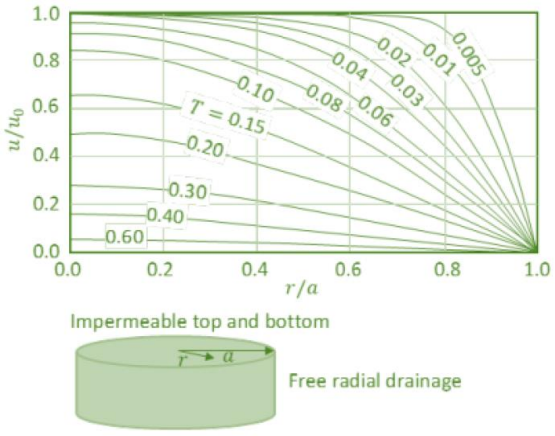

Figure 1. Pore pressure dissipation in a disk with radial drainage (from Andersen, 2015); Normalised drainage time, T, derived as per Equation 1 below

$$T = \frac{c_v}{\alpha^2} \cdot t \qquad (1)$$

where T is the normalised drainage time and c_v (m^2/s) is the consolidation coefficient.

3 FEA MODEL

3.1 FEA Cases

The base case (Case 1) is a uniform profile of dense clean sand with monopile embedment ratio (L/D) of 3.2 and a coefficient of permeability (k) of 5e-5 m/s. Cases 2 and 3 differ only in terms of L/D, with values of 2.7 and 4.2, respectively. Case 4 is like Case 1 with the difference that k is 1e-6 m/s representing a dense silty sand. Case 5 introduces a shallow clay layer in the top 5 m of the profile. The clay is modelled as practically impermeable (k=1e-10 m/s). Figure 2 presents a schematic of the considered FEA cases.

Figure 2. Schematic of FEA cases

3.2 Model Set-up

The full 3D FE mesh of both the soil and the pile was developed using 10-noded quadratic fully integrated tetrahedral elements. Each FE model comprised half of the pile and soil considering the symmetry of the laterally loaded monopile problem. All vertical boundaries (including the plane of symmetry) were normally fixed and the lower horizontal boundary was fully fixed. All ground water flow boundaries were open except for the plane of symmetry and the lower horizontal boundary. Six-noded triangular shell elements were used to model the steel pile wall. The pile steel was represented using a linear elastic model with a Young's modulus of 210 MPa and Poisson's ratio of 0.3. Between the pile wall and the soil, 12-noded interface elements were used to model soil-structure interaction. The interface elements were modelled with an elastic stiffness of 10^5 kN/m^3 and a strength of 2/3 the strength of the adjacent soil.

The element distribution across the mesh was optimised to provide local refinement in the zones close to the pile shaft and tip, while limiting the number of elements in the outer zones of the model. Following a mesh sensitivity analysis to determine the optimal

mesh density and configuration while balancing analysis calculation times and accuracy, the following model dimensions were considered:

- 2.5 pile embedded lengths horizontally in the direction and opposite to the direction of loading.
- 3.5 pile diameters horizontally perpendicular to the direction of loading.
- 1.7 pile embedded length for the bottom vertical boundary.

The FEA considered a pile diameter of 10 m with a pile wall thickness of 72 mm. Isotropic permeability was assumed in all analyses.

The FEA model included four calculation stages:

- Initial: isotropic conditions were assumed (coefficient of earth pressure at rest, $K_0 = 1$).
- Pile installation: pile wished in-place (the contribution of installation effects to the overall drainage capacity of the soil-monopile model was assessed by the authors as minor).
- Horizontal loading: consolidation analysis with simultaneous application of the prescribed monopile loads within a time interval of 2.5 seconds, simulating one quarter of a cycle with a loading frequency of 0.1 Hz.
- Consolidation: consolidation analysis for a time interval of 1,000 seconds, simulating the time required for 100 storm loading cycles with a frequency of 0.1 Hz.

An undrained pushover analysis was performed for each of the five cases to determine the failure load. Two load utilisations were considered, i.e. 50 % of the failure (ultimate) load, targeting normal operating conditions, and 90 % of the failure load, targeting extreme close-to-failure conditions. A lever arm of 52 m was assumed. Table 1 presents the failure load utilisations for each case.

Table 1. Failure load utilisations

Case	Horizontal Load [MN]	
	50 % utilisation	90 % utilisation
1	9.90	17.82
2	6.35	11.43
3	23.95	35.00
4	9.90	16.93
5	9.83	16.81

3.3 Soil Constitutive Model

The aim was to calibrate the soil constitutive model against cyclic contour diagrams to represent adequately both the cyclic pore pressure development and shear stress-strain response for a specific number of cycles (i.e. N_{eq} curve). The cyclic contour diagrams that were selected to calibrate the model were taken from a typical North Sea sand unit corresponding to the Yarmouth Roads formation.

For the selection of N_{eq} for which to derive envelope stress-strain and excess pore pressure-strain curves, a few North Sea storms from the authors' internal database and past experience have been considered and a value of N_{eq}=50 was selected as representative of the degradation expected in a sand unit after the peak storm excluding any drainage effects, i.e. under fully undrained conditions.

The Modified Cam-Clay (MCC) model (Muir Wood, 1991) was selected due to its ease for calibration, good performance against the cyclic contour diagram plots (Figure 3) and considering that the flow rule of the MCC model has been shown to perform well in predicting the volumetric accumulation in cyclic testing (Wichtmann, 2016), which manifests as excess pore pressure in undrained cyclic loading. Figure 3 presents a comparison of a single element test simulation (undrained DSS test) with the calibrated MCC model against the envelope (N_{eq}=50) pore pressure ratio curve from the cyclic contour diagrams selected from our database.

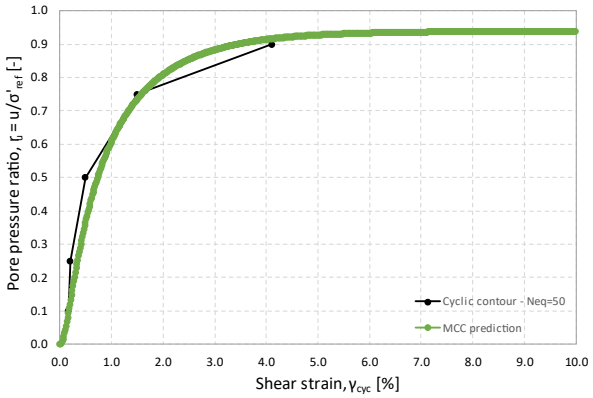

Figure 3. Pore pressure ratio versus shear strain

The MCC yield function was slightly modified to better capture the N_{eq} envelope stress-strain and excess pore pressure generation response (Equation 2).

Table 2 summarises the calibrated MCC model parameter values. These values also apply to the clay layer modelled in Case 5 to ensure comparable stiffness with the other cases and minimise influence on the drainage results.

$$f = \frac{q^2}{M^2} + 2p'(2p' - p_c) \qquad (2)$$

Table 2. MCC calibrated parameter values

Model Parameter	Description	Value
λ	Cam-Clay compression index	0.12
κ	Cam-Clay swelling index	0.01
M	Tangent of the critical state line	0.69-0.93
e_{ini}	Initial void ratio for loading/unloading	0.59
v_{ur}	Poisson's ratio	0.30

4 RESULTS

4.1 General

It can be seen from Figure 4 that the drainage time below the monopile pivot point (i.e. the deep failure zone within bottom ~0.3L of the monopile) and around the pile base is significantly shorter than within the wedge mechanism (shallow failure zone top ~0.5L of the monopile). This observed behaviour is according to expectations when considering the difference in the relative drainage paths of the excess pore pressure generated within the shallow mechanism and the deeper mechanism of a laterally loaded monopile. At the base of the pile drainage can occur upwards within the plug and downwards to deeper soil with a shorter drainage path than within the shallow wedge failure mechanism where radial drainage is predominant. In addition, the toe failure mechanism is more localised and hence shorter drainage paths occur.

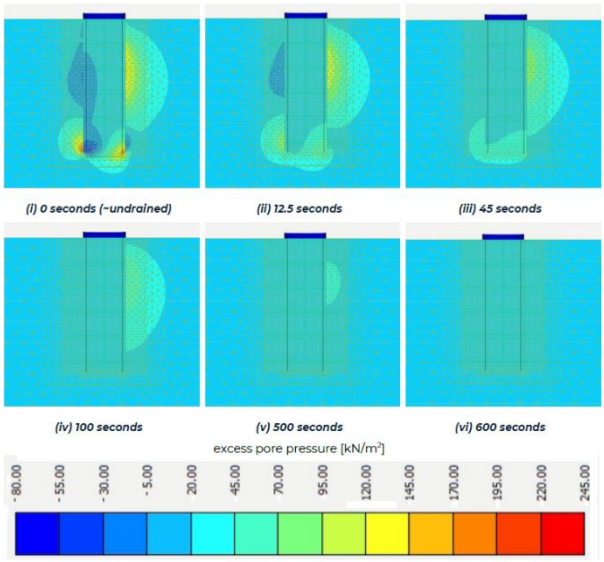

Figure 4. Excess pore pressure contours at different time intervals – Case 1 at 50 % ultimate load utilisation

4.2 Statistical Approach

A statistical approach was adopted whereby the excess pore pressure at all stress points of the mesh was extracted and post-processed through a python script. Figure 5 illustrates an example showing the excess pore pressure around the monopile at the end of the horizontal loading stage. The same pore pressure bulbs (zones where the excess pore pressure is larger), as presented in Figure 4(i), are evident.

In order to increase the robustness of the statistical analysis, a number of criteria were applied to the extracted excess pore pressure results at the stress points. If at start of consolidation the pore pressure ratio $r_u = u/\sigma'_v \leq 0.1$, it was considered negligible and the stress point was excluded from further analysis. If at any time during consolidation $r_u \leq 0.1$, then the PPR of the stress point was set to zero, i.e. the point is considered to be drained.

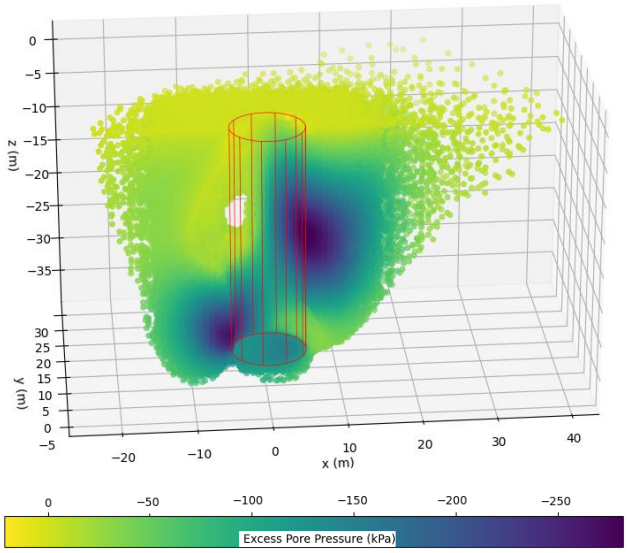

Figure 5. Post-processed stress points showing excess pore pressure at the end of the horizontal loading stage – Case 1 at 90 % ultimate load utilisation

The normalised cumulative histograms of the PPR at various time intervals during consolidation were then determined (Figure 6 presents an example for Case 2). The median PPR for each histogram was selected as an indicative measure of the system drainage and was used to determine an average drainage length for use in the analytical dissipation model (see Section 2).

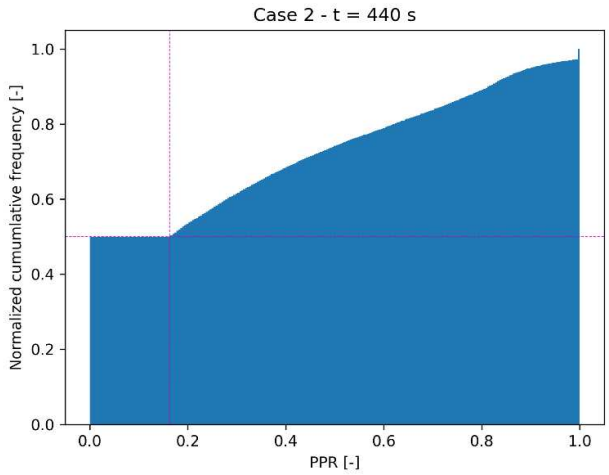

Figure 6. Normalised cumulative histogram of PPR for Case 2 at the time of nearly full drainage – 50 % ultimate load utilisation (pink dashed line is the median PPR)

Figure 7 and Figure 8 present the evolution of the median PPR versus consolidation time per case, for the 50 % and 90 % ultimate load utilisations, respectively.

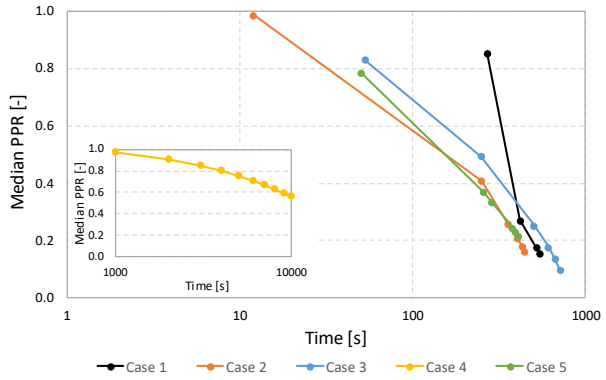

Figure 7. Median PPR versus consolidation time per case – 50 % ultimate load utilisation

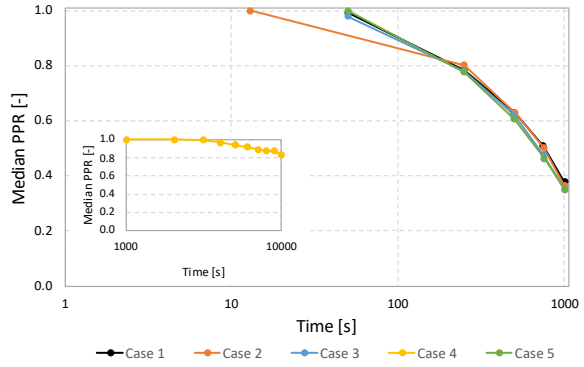

Figure 8. Median PPR versus consolidation time per case – 90 % ultimate load utilisation

To estimate the drainage length an estimation of the consolidation coefficient (c_v) is required. This was done considering 1D vertical consolidation in accordance with the following equation:

$$c_v = \frac{k \cdot M}{\gamma_w} = \frac{k}{\gamma_w} \cdot \frac{(1+e) \cdot \sigma'_{v0}}{\lambda} \quad (3)$$

Figure 9 presents the derived normalised drainage lengths per case and per load utilisation. Note that these are radial drainage lengths applicable to the Andersen (2015) analytical dissipation model.

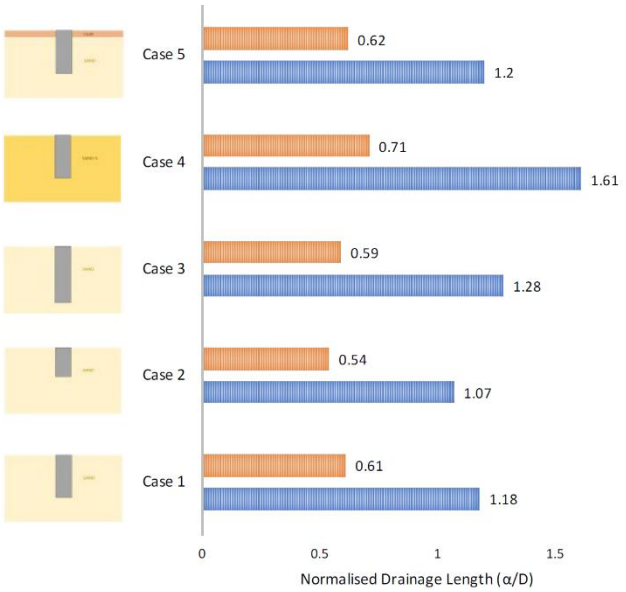

Figure 9. Normalised drainage lengths per case for two load utilisations (orange: 50 %; blue: 90 %)

5 DISCUSSION

Figure 9 illustrates that the drainage length for the 5 cases analysed ranges between ~0.5D and ~1.3D (where D is pile diameter) depending on the case and the ultimate load utilisation. As expected, larger load utilisations lead to larger generation of excess pore pressures which take longer to dissipate thus increasing the back-figured radial drainage lengths. The range of drainage lengths between the cases is relatively narrow with a mean value of 0.61 and standard deviation of 0.06 at 50 % ultimate load utilisation (relevant for SLS loading conditions), and a mean value of 1.27 and standard deviation of 0.21 at 90 % ultimate load utilisation (relevant for ULS loading conditions). The drainage lengths as outlined in Figure 8 are generally in line with the pore pressure bulb lengths, which are ≤1.0D, as seen for example for Case 1 in Figure 4.

Figure 8 shows that the drainage length does not vary much with L/D (Cases 1, 2 and 3) provided that the monopiles are loaded to the same utilisation. This is also evident from review of the median PPR evolution with time (Figure 6 and Figure 7) where a similar trend is observed; particularly at 90 % utilisation the PPR curves fall practically on top of each other for Cases 1, 2 and 3. This shows that there

are two factors with reverse effect that are influencing drainage in piles of differing length:

- As L/D increases and the load utilisation stays the same, the monopile imposes a larger mobilisation to the soil around it and hence a larger generation of excess pore pressures that should consequently increase the system drainage time and the back-calculated drainage length. This L/D trend is mainly due to the observed drainage behaviour of the shallow wedge mechanism where drainage is predominantly radial. At larger depths near the pile toe, it is shown that drainage occurs relatively quickly irrespective of the different excess pore pressure generation from the piles with different L/D ratio (Figure 10).
- As the monopile length increases, there is greater availability of drainage paths for (vertical and radial) dissipation of the generated excess pore pressures due to the contribution of a larger proportion of the mesh to the drainage process, therefore it tends to decrease the system drainage time and the back-calculated drainage length.

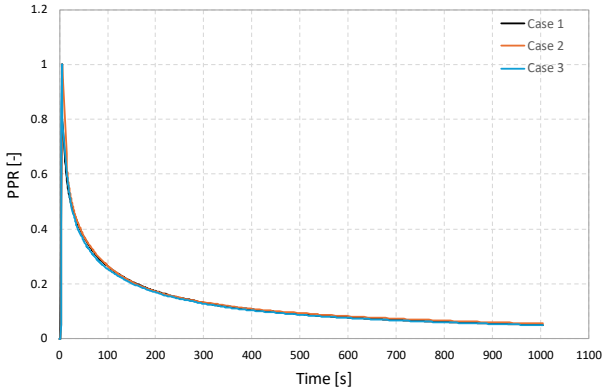

Figure 10. PPR versus time for Cases 1, 2 and 3 at 90 % ultimate load utilisation – Stress point at 1 m away from the pile sleeve at the back face of the pile toe

From review of the median PPR evolution with time (Figure 7 and Figure 8) for Case 4, it can be deduced that the behaviour can be considered fully undrained since after 1000 seconds following load application (i.e. a time interval that can be translated to 100 load cycles with frequency of 0.1 Hz), no significant excess pore pressure dissipation has taken place, i.e. median PPR is unity. The dissipation time needs to be extended tenfold to reach some noticeable pore pressure dissipation, i.e. median PPR at 50 % ultimate load utilisation is 0.56 after 10,000 seconds. It has been therefore shown that silty sand layers with coefficient of permeability as low as 1e-6 m/s (Case 4) will likely behave fully undrained during cyclic accumulation with no or very little partial drainage during application of the storm cyclic load history. To showcase the significant effect of the sand permeability on the excess pore pressure dissipation, an alternative Case 4 with 5 times higher coefficient of permeability (k=5e-6 m/s) was run and the evolution of the median PPR versus consolidation time for the 50 % ultimate load utilisation is presented in Figure 11 for comparison.

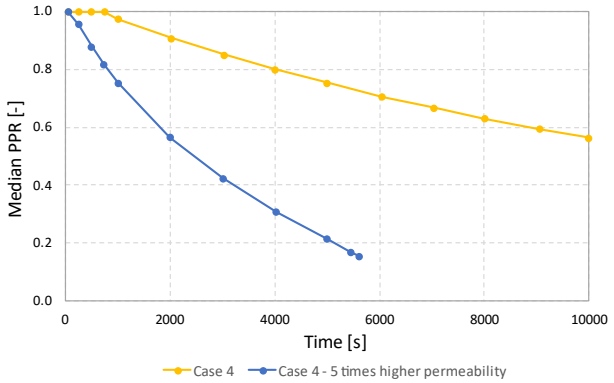

Figure 11. Median PPR versus consolidation time for Case 4 and an alternative Case 4 with higher permeability – 50 % ultimate load utilisation

The presence of a shallow (practically impermeable) clay layer that is generally thin relative to the PPD does not seem to have a significant impact on the overall drainage capacity of the monopile-soil model (see Case 1 and Case 5 results in Figure 8). Similar time-domain numerical analyses in the literature confirm the above outcome (Chaloulos et al., 2024). This is according to expectations after review of the drainage mechanisms around a laterally loaded monopile:

- The drainage mechanism at the deep failure zone near the pile toe involves significant vertical drainage towards deeper soil and the soil plug which is not particularly hindered by the presence of shallow impermeable layers.
- The predominant drainage mechanism at the shallow wedge failure mechanism is radial drainage which is also not hindered by the presence of shallow impermeable layers.

6 CONCUSION AND RECOMMENDATIONS

The excess pore pressure development and dissipation (i.e. drainage response) around a monopile under lateral loading is highly complex, as shown by the results presented within this study, and therefore the development of simple generic design rules is challenging. The numerical analyses performed and presented herein provide further insight in the expected drainage response for laterally loaded monopiles in sandy soils. It

has been shown that the drainage characteristics of the system can have a substantial impact on monopile response. The amount of drainage in sandy soils under cyclic loading directly affects the design PPD; therefore, representative consideration of the system drainage response is key to ensure a safe and optimised monopile design.

The premises and assumptions of this study must be noted though. In particular, the drainage results are sensitive to the monopile mobilisation, therefore sensitive to the strength and stiffness characteristics of the cyclic contours that were used in this study to calibrate the constitutive model against. An additional study, expanding on the results of the current one, is recommended to derive more systematic results by consideration, for example, of a larger pool of soil cyclic contours, pile geometrical configurations and loading conditions, that would further span the parametric space of the parameters likely to influence drainage during cyclic lateral loading of monopiles. Nevertheless, this study made an important first step into providing insight in the representation of the drainage response expected for laterally loaded monopiles in the sandy soils along with some guidance in the parameter selection (e.g. drainage length) used in simplified design procedures (e.g. Andersen, 2015).

AUTHOR CONTRIBUTION STATEMENT

K. Kaltekis: Formal Analysis, Investigation, Methodology, Supervision, Validation, Writing – Original draft. **C. Piatti**: Data curation, Formal Analysis, Software, Visualization. **S. Whyte**: Supervision, Validation, Writing – Reviewing and Editing. **E. Skoufaki, L.R. Christiansen**: Funding acquisition.

ACKNOWLEDGEMENTS

The authors are grateful for the financial support provided by Vattenfall for conceptualising and performing this numerical study.

REFERENCES

Andersen, K. (2015). Cyclic soil parameters for offshore foundation design. *Proceedings of the International Conference Frontiers in Offshore Geotechnics III, ISFOG'2015,* Meyer (Ed). Taylor & Francis Group, London, Vol. 1, pp. 5-82.

Chaloulos, Y., Tasiopoulou, P., Giannakou, A., Chacko, J., Aghakouchak, A. and Stergiou, T. (2024). Fully-Coupled cyclic time-history analyses of monopile foundations in sand. *Ocean Engineering*, vol. 298. https://doi.org/10.1016/j.oceaneng.2024.116691

Muir Wood, D. (1991). *Soil Behaviour and Critical State Soil Mechanics*. University of Glasgow, Cambridge University Press. https://doi.org/10.1017/CBO9781139878272

Plaxis (2021). PLAXIS CONNECT Edition V22.00. Bentley, Delft, The Netherlands.

Wichtmann, T. (2016). *Soil behaviour under cyclic loading – experimental observations, constitutive description and applications*, Habilitation Thesis, Karlsruher Institut für Technologie (KIT).

INTERNATIONAL SOCIETY FOR SOIL MECHANICS AND GEOTECHNICAL ENGINEERING

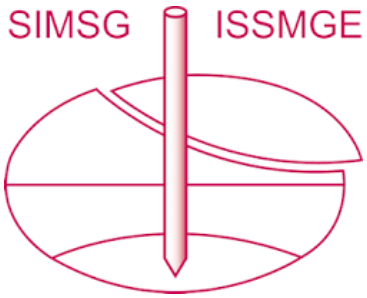

This paper was downloaded from the Online Library of the International Society for Soil Mechanics and Geotechnical Engineering (ISSMGE). The library is available here:

https://www.issmge.org/publications/online-library

This is an open-access database that archives thousands of papers published under the Auspices of the ISSMGE and maintained by the Innovation and Development Committee of ISSMGE.

The paper was published in the proceedings of the 5th International Symposium on Frontiers in Offshore Geotechnics (ISFOG2025) and was edited by Christelle Abadie, Zheng Li, Matthieu Blanc and Luc Thorel. The conference was held from June 9th to June 13th 2025 in Nantes, France.